Optical and hygroscopic properties of Asian dust particles based on a horizontal Mie lidar: case study at Hefei, China

Guangyu Bo (伯广宇)[1], Chidong Xu (徐赤东)[2,*], Aiyue Li (李爱悦)[2], Yanfei Wang (王燕飞)[2], Haiyan Chen (陈海燕)[1], and Yuqiang Jiang (姜育强)[1]

[1]*Institute of Technology Innovation, Hefei Institutes of Physical Science, Chinese Academy of Sciences, Hefei 230031, China*

[2]*Center of Medical Physics and Technology, Hefei Institutes of Physical Science, Chinese Academy of Sciences, Hefei 230031, China*

**Corresponding author: cdxucas@126.com*

Received October 16, 2016; accepted December 15, 2016; posted online January 16, 2017

As an extension of the Mie lidar technique to measure the extinction coefficient of the surface particles, a horizontally pointing Mie lidar is used for determining the optical properties of Asian dust, which is an approach without knowing the actual lidar ratio. A long lasting dust event is observed based on this approach in May 2014. The "no dust," "pure dust," and "polluted dust" stage is observed during this event, and their optical and hygroscopic properties are discussed. Some new optical and hygroscopic features are observed, which benefit from the quantitative, multi-wavelength, and continuous measurement of the extinction related optical properties of dust particles.

OCIS codes: 010.0010, 140.0140, 280.0280, 290.2200.
doi: 10.3788/COL201715.020102.

Asian dust generated in the Taklimakan and Gobi deserts is one of the major dust systems in the world and significantly affects the climate system in East Asia[1]. Quantitatively observing the extinction coefficient of dust particles could minimize the uncertainty in predicting aerosol radiative properties with models. Unfortunately, most observations in East Asia are concerned with the dust backscatter coefficient from using the Mie lidar[2], where only a few studies reported the extinction coefficient by using the Raman or high spectral resolution lidar. Thus, the characteristics of the dust extinction coefficient in East Asia are still not well-known.

Compared to the Raman and high spectral resolution lidar, Mie lidars are more common instruments in China and should be a useful candidate for the observation of Asian dust. For a vertically pointing Mie lidar, the unknown lidar ratio is a key parameter for the retrieval of the aerosol extinction coefficient. However, previous research has found that the lidar ratio of dust can vary between 20 and 100 sr[3], depending on its originating sources and dust–pollutant mixing state. Therefore, without knowing the actual lidar ratio, it is difficult to accurately measure the dust extinction coefficient with a vertically pointing Mie ldar.

Most lidars are used to observe the vertical distributions of aerosols[4,5]. However, due to the influence of the lidar's blind zone, a vertically pointing lidar is difficult to use to observe the surface aerosols. Generally, dust storms moving near the surface are more directly affected by anthropogenic pollutants. It is an interesting subject if we just focus on the surface particles for a better understanding of the dust–pollutant mixing process. Under this circumstance, both the lidar ratio and the lidar's blind zone problem that were mentioned earlier can be avoided by using a horizontally pointing Mie lidar[6–8].

The objective of this study is to investigate the optical properties of surface dust by using a horizontally pointing Mie lidar. The lidar system is based on an Nd:YAG laser with a 1064 and 532 nm wavelength with both having a transmitted energy of 100 mJ per pulse at a pulse repetition laser frequency of 20 Hz. The lidar signal was received by two channels at 532 nm and a third channel at 1064 nm through a 200 mm diameter telescope. The signals were recorded with a temporal resolution of 5 min and a spatial resolution of 7.5 m. Two wavelength extinction coefficients at 532 and 1064 nm, where the particle's depolarization ratio (DR) is 532 nm, and the extinction related Ångstrom exponent (AE)[9] have been observed, while the data processing methods of the horizontally pointing lidar can be found in Ref. [7]. The characteristic of the particle hygroscopic properties during a dust event was also investigated based on the synchronous measurement of the particle's optical properties and atmospheric relative humidity (RH). All of the times in this Letter, unless otherwise stated, are given in China Standard Time, which is 8 h ahead of the Coordinated Universal Time (UTC).

We focus on a dust event passing through Hefei, China in May 2014. Figure 1 shows the 72 h backward trajectories for the layers at 100, 200, and 500 m in Hefei calculated with the Hybrid Single Particle Lagrangian Integrated Trajectory model (HYSPLIT)[10]. The dust event could be traced back to the Taklamakan and Gobi deserts before being transported to east China[11]. This dust event was also observed in western Japan[12]. The aerosol spatial distribution measured by Moderate Resolution Imaging Spectroradiometer (MODIS), and the

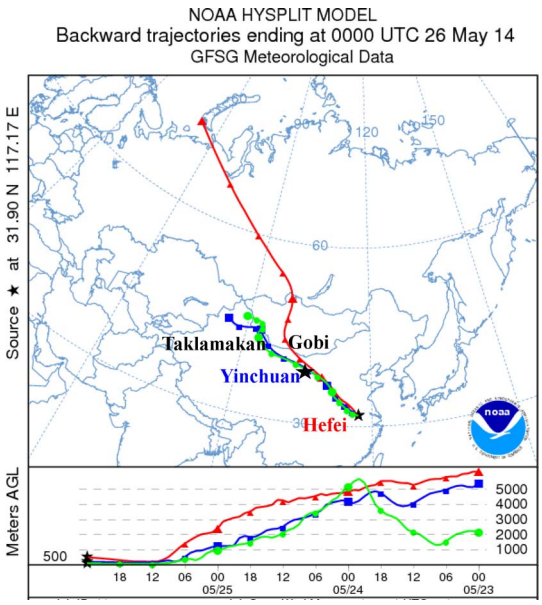

Fig. 1. 72 h backward trajectories in Hefei.

meteorological fields over East Asia during the dust event can be found in Refs. [11,12].

Figure 2 gives the time series for the 1 h average aerosol mass concentrations (MCs, measured by a tapered element oscillating microbalance) during the observation period. As we can see from Fig. 2, the average MC of fine particles (diameter < 2.5 μm) and coarse particles (diameters between 2.5 and 10 μm) reached 41.2 ± 12.6 and 28.4 ± 14.4 μg/m^3 before May 26, which is maintained at the background levels in the Hefei area.

After the first dust plume arrived in the observation site at about 00:00 May 26, the aerosol MC of the fine and coarse modes show a coinciding increase trend with the peak value reaching129 and 300 μg/m^3, respectively. The average MC of fine and coarse particles during the dust intrusion period was 84.3 ± 22.5 and 154.9 ± 64.9 μg/m^3, which was much higher than that of the background levels at Hefei.

Figure 3 presents the extinction coefficient, AE, and DR measured from 00:00 May 24 to 00:00 May 31. The simultaneously observed RH at the ground was also given in Fig. 3, where it is noticeable that RH was not present after 10:15 May 30 because of the RH sensor maintenance.

The DR served as a key parameter for classifying spherical or non-spherical particles. According the previous

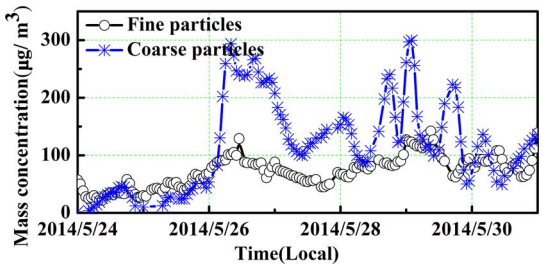

Fig. 2. Time series of the particle mass MC during observation.

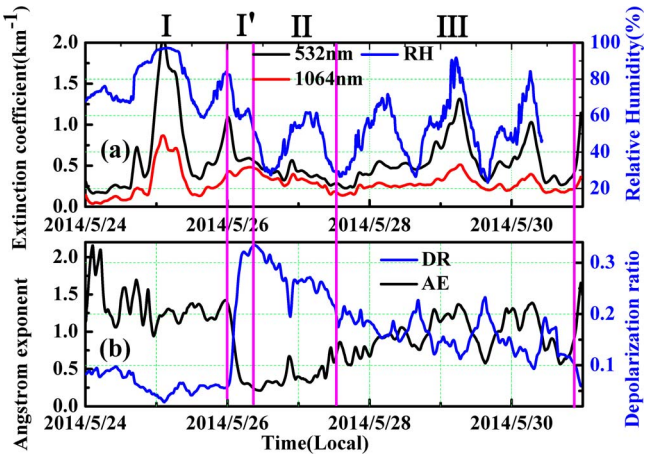

Fig. 3. Temporal evolution of aerosol optical properties and RH during the observation.

studies in East Asia, we used DR > 0.1 as a threshold to identify whether the aerosols carried dust composition[13], and DR > 0.2 to classify the pure Asian dust[13–15]. Between the spherical and pure dust, the DR strongly depends on the mixing ratio of the dust and spherical particles. Based on the observed DR value, we classified the whole observation into three periods (Period I, II and III), as shown in Fig. 3.

In Period I (before 00:00 May 26), the observed DR varied from 0.029 to 0.1 with an average value of 0.064 ± 0.018, and the observed AE spread of from 0.9 to 2.2 with a mean value of 1.35 ± 0.25. The low DR associated with the high AE indicates a size distribution dominated by spherical and fine-mode particles, this period was designated as the "no dust period." Despite the lowest MC (see Fig. 2), this period featured the highest extinction coefficient of 2.03 km^{-1} (532 nm) and 0.87 km^{-1} (1064 nm) at a high RH value of 97%, indicating that the hygroscopic growth of particles exerts a strong influence on the light extinction.

After 00:00 May 26, a dramatic shift in the aerosol optical properties occurred. The observed DR increased from 0.058 to 0.33, meanwhile the AE decreased from 1.39 to 0.23, indicating that the aerosol particle size shifted quickly from fine mode to coarse mode. This period was designated as the transitional period from "no dust" to "pure dust" and was denoted as Period I'. A simultaneous decrease of the extinction coefficient and RH was observed in this period, indicating that the hydrophobic dust and dry air flows were simultaneously transported to the observation site. In the combined effect of the falling RH and the lack of hydrophilic particles, the extinction coefficient at both wavelengths decreased despite the rapid increase of the aerosol MCs.

In Period II (09:00 May 26 to 12:50 May 27), the observed DR decreased from 0.33 to 0.2 (mean value: 0.27 ± 0.03), and the AE increased from 0.23 to 0.7 (mean value: 0.40 ± 0.14), such a low AE and high DR indicates that this period was governed by dust particles. We

Table 1. The Measured Aerosol Optical Properties During the Three Periods

Item		Period I (No Dust Period)	Period II (Pure Dust Period)	Period III (Polluted Dust Period)
DR	Range	0.029–0.1	0.33–0.2	0.09–0.23
	Average	0.064 ± 0.018	0.27 ± 0.03	0.16 ± 0.03
AE	Range	0.9–2.2	0.23–0.7	0.55–1.39
	Average	1.35 ± 0.25	0.40 ± 0.14	0.95 ± 0.23
Extinction coefficient at 532 nm (km^{-1})	Range	0.16–2.02	0.26–0.57	0.23–1.31
	Average	0.66 ± 0.53	0.41 ± 0.08	0.54 ± 0.24
Extinction coefficient at 1064 nm (km^{-1})	Range	0.04–0.87	0.15–0.47	0.14–0.51
	Average	0.28 ± 0.23	0.31 ± 0.07	0.27 ± 0.08

designated this period as the "dust dominant period". The decreasing trend of the DR and the increasing trend of the AE during this period also suggested that the dust storm was gradually weakened. The extinction coefficient was also decreased from approximately 0.57 to 0.26 km^{-1} (mean value: 0.41 ± 0.08 km^{-1}) at 532 nm, and 0.47 to 0.15 km^{-1} (mean value: 0.31 ± 0.07 km^{-1}) at 1064 nm.

In Period III (12:50 May 27 to 21:20 May 30), the observed values of the AE and DR shows a fluctuation from 0.55 to 1.39 (mean value: 0.95 ± 0.23) and 0.09 to 0.23 (mean value: 0.16 ± 0.03), respectively. The extinction coefficient fluctuated between 0.23 and 1.31 km^{-1} (mean value: 0.54 ± 0.24 km^{-1}) at 532 nm and 0.14 to 0.51 km^{-1} (mean value: 0.27 ± 0.08 km^{-1}) at 1064 nm. The optical properties show an obvious dependence on the RH, which could be caused by the dust particles' simultaneous transport with the hydrophilic pollutants. This period was given as the "polluted dust period."

To present the difference of the optical properties during the three periods visually and exactly, the detailed values of the observations are listed in Table 1.

Followed by Period III, a decreasing trend of the DR (down to 0.054 at 00:00 May 31) and an increasing trend of the AE (up to 1.65 at 00:00 May 31) can be observed, indicating that the dust particles have almost dispersed at 00:00 on May 31.

To investigate the correlation trends between the DR and AE during this dust event, Fig. 4 shows the scatter plot between the DR and AE (without the transitional period, i.e., Period I). The dramatic change of the AE (0.23–2.2) and the DR (0.029–0.33) reflected the significant variation of the aerosol microphysical and/or chemical properties during the observation period.

The data points of the dust dominant particles (Period II) are in the upper-left portion of Fig. 4, and clearly separate from the data points of the polluted particles in the lower-right portion (Period I). Data clusters connecting Periods I and II reflect the mixing process of dust with pollutants. We note that the AE were negatively correlated with the DR in Periods II and III, implying that the particle non-sphericity increased with an increase in the particle size. No correlation between the AE and the DR can be found in Period I.

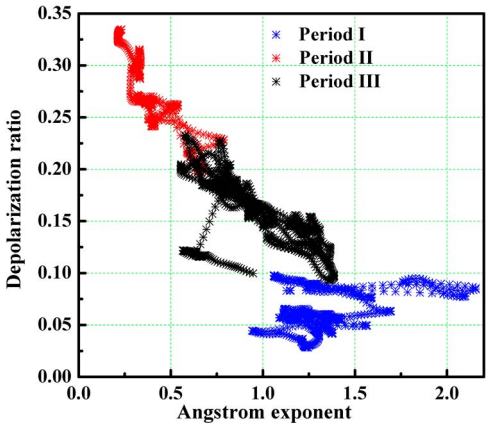

Fig. 4. Scatter diagram between the AE and the DR at 532 nm.

Pure dust does not absorb water because they were hydrophobic, but it may become hydrophilic if mixed with hydrophilic particles. Few studies have reported the hygroscopic properties of dust particles. In this section, we will focus on the particle hygroscopic growth properties during the dust–pollutant mixing period. It should be noted that under ambient atmospheric conditions, the changes in the aerosol extinction coefficient could be caused by variations in the particle size distribution, or RH, or other related factors. As a result, we confined to qualitative analysis of the hygroscopic properties. If the relation between extinction and RH is positively correlated, it indicates that some of the observed variability in the extinction coefficient may be attributed partially to the hygroscopic growth. A correlation of the extinction coefficient at 532 nm and the RH is shown in Fig. 5.

In Period I, a relatively high RH (~97%) was observed, a positive correlation (correlation coefficient $R = 0.65$) can be found between the extinction coefficient and RH, indicating a strong hygroscopicity of particles, which could be the background pollutant in the Hefei area. In Period II, a moderately high RH (~61%) was measured, and no

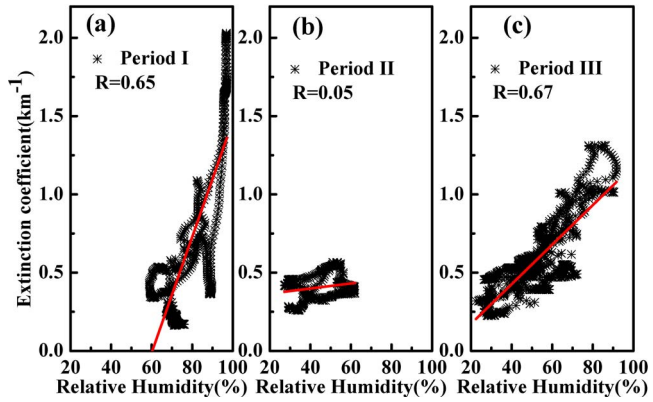

Fig. 5. Extinction coefficient in relation to the RH.

correlation ($R = 0.05$) between the extinction coefficient and RH can be found, indicating that the mineral dust was primarily hydrophobic. In Period III (before 10:15 May 30), the extinction coefficients was positively correlated with the RH ($R = 0.67$), indicating that the dust was mixed with hydrophilic aerosols (could be pollutant particles) during its transportation.

Generally, the DR of hydrophilic particles would decrease with an increasing RH, which suggests an increase in the particle sphericity. Meanwhile, under an assumption of the Junge particle size distribution, the AE would decrease with an increasing RH, which suggests an increase in the aerosol particle size[16]. Figure 6 gives the scatter plots of the DR and AE as a function of the RH. In Period I, the DR shows a weak negative correlation ($R = 0.35$) with the RH. The possible reasons for this negative correlation were: the non-spherical particles changed their shape to be spherical by up-taking water vapor, and/or the proportion of the non-spherical particles to the other low-depolarizing particles decreased with an increasing RH. A clear trend cannot be deduced between the AE and RH during Period I.

In Period II, no correlation can be found between the AE ($R = 0.004$) and the RH or the DR ($R = 0.03$) and the RH, indicating that hygroscopic growth of pure dust was substantially suppressed. In Period III, the DR

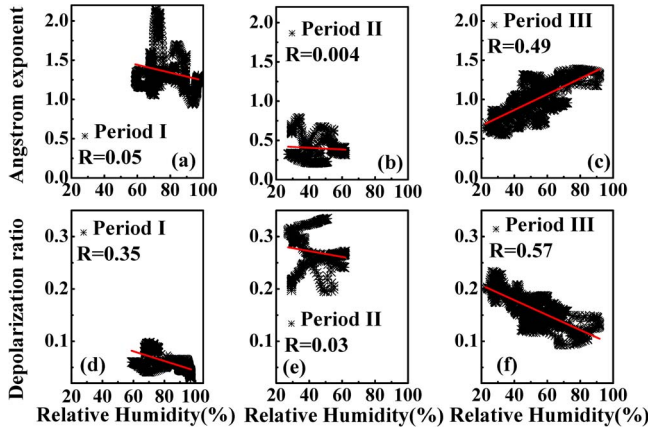

Fig. 6. DR and AE in relation to the RH.

($R = 0.57$) showed a negative dependence on the RH; this was related with the hygroscopic growth effect of the polluted dust. Surprisingly, a positive correlation between the AE ($R = 0.49$) and RH was observed during Period III. Loeb *et al.* has modeled the hygroscopic growth of a bimodal particle size distribution. Their result shows that a bimodal particle size distribution with a hygroscopic fine mode (such as a pollutant) and a hydrophobic coarse mode (such as dust) can produce increases in the AE as the fine mode swells[17].

In conclusion, the extinction related optical properties during a typical dust event are quantitatively recorded and discussed. The observation results indicate that the horizontal Mie lidar can be used to measure the dust optical properties with high precision. We also discuss the particle hygroscopic properties using optical parameters measured in the ambient RH conditions. Distinguishable differences in the optical and hygroscopic properties between pure dust and polluted dust are observed. As a result, we generally treat the polluted dust as pure dust, which can cause huge errors in estimating their climate forcing effect. Future observations are still required to provide more valuable information about dust extinction properties.

This work was supported by the National Natural Science Foundation of China under Grant Nos. 41205019 and 41665001. We also thank Dr. Xiaoqing Wu, Dr. Chenbo Xie, and Dr. Guangqiang Fan for providing the aerosol mass concentration and the meteorological data.

References

1. J. Li, Z. Wang, G. Zhuang, G. Luo, Y. Sun, and Q. Wang, Atmos. Chem. Phys. **12**, 7591 (2012).
2. N. Sugimoto, T. Nishizawa, A. Shimizu, I. Matsui, and H. Kobayashi, J. Quantum Spectrosc. Radiat. Transfer **150**, 107 (2015).
3. Z. Liu, D. Winker, A. Omar, M. Vaughan, C. Trepte, Y. Hu, K. Powell, W. Sun, and B. Lin, J. Quantum Spectrosc. Radiat. Transfer **112**, 204 (2011).
4. Z. Chen, W. Liu, Y. Zhang, and B. Heese, Chin. Opt. Lett. **10**, S10101 (2012).
5. L. Lv, W. Liu, G. Fan, T. Zhang, Y. Dong, Z. Chen, Y. Liu, H. Huang, and Y. Zhou, Chin. Opt. Lett. **14**, 060101 (2016).
6. J. N. Porter, B. Lienert, and S. K. Sharma, J. Atmos. Oceanic Technol. **17**, 1445 (2000).
7. B. Guangyu, L. Dong, W. Decheng, and Z. Zhiqing, Chin. J. Lasers **41**, 0113001 (2014).
8. G. J. Kunz and L. G. De, Appl. Opt. **32**, 3249 (1993).
9. A. Ångstrom, Tellus **16**, 64 (1964).
10. R. R. Draxler and G. D. Rolph, *Hysplit (HYbrid Single Particle Lagrangian Integrated Trajectory) Model* (NOAA Air Resources Laboratory, 2012).
11. F. Wang, Z. Zhong, S. Wu, W. Zhang, Q. Li, S. Hu, and J. Wang, Acta Scientiarum Naturalium Universitatis Pekinensis **51**, 1132 (2015).
12. X. Pan, I. Uno, Y. Hara, M. Kuribayashi, H. Kobayashi, N. Sugimoto, S. Yamamoto, T. Shimohara, and Z. Wang, Geophys. Res. Lett. **42**, 1593 (2015).

13. A. Shimizu, N. Sugimoto, I. Matsui, K. Arao, I. Uno, T. Murayama, N. Kagawa, K. Aoki, A. Uchiyama, and A. Yamazaki, J. Geophys. Res. Atmos. **109**, 1255 (2004).
14. Z. Liu, T. Duncan Fairlie, I. Uno, J. Huang, D. Wu, A. Omar, J. Kar, M. Vaughan, R. Rogers, D. Winker, C. Trepte, Y. Hu, W. Sun, B. Lin, and A. Cheng, J. Quantum Spectrosc. Radiat. Transfer **116**, 24 (2013).
15. B. Yi, P. Yang, and B. A. Baum, J. Geophys. Res. Atmos. **119**, 5397 (2014).
16. M. J. Granados-Muñoz, F. Navas-Guzmán, J. A. Bravo-Aranda, J. L. Guerrero-Rascado, H. Lyamani, A. Valenzuela, G. Titos, J. Fernández-Gálvez, and L. Alados-Arboledas, Atmos. Meas. Tech. Discuss. **7**, 10293 (2014).
17. N. G. Loeb and G. L. Schuster, J. Geophys. Res. **113**, 762 (2008).